ROYAL SOCIETY
OF CHEMISTRY

Check for updates

Sustainable low-cost carbon fibres produced by integrating wood fractionation with lignin fibre spinning†

Shirley Min Yang,‡[a] Rukayya Ibrahim Muazu,‡[b] Enny Tran, [c] Clifford B. Talbot,[d] Nilay Shah,[b] Milo S. P. Shaffer [ac] and Agnieszka Brandt-Talbot [*a]

Conventional carbon fibre manufacturing is costly and relies on fossil-based raw materials with significant environmental impacts. This study presents a new, low-cost route to biobased carbon fibres generated directly from wood by integrating ionosolv wood fractionation with carbon fibre spinning. The approach avoids isolating lignin powders by spinning lignin directly from the black liquor, offering a simpler process with a lower environmental impact. The concept is demonstrated using lignin extracted from eucalyptus wood into the recyclable ionic liquid (IL) *N,N*-dimethylbutylammonium hydrogen sulfate with 20% water, generating delignified cellulose pulp as a co-product. After adding non-toxic poly(vinyl alcohol) (PVA) into the lignin-containing ionic liquid (with up to a 4.7 : 1 lignin : PVA ratio) continuous lignin−PVA fibres were generated by spinning into an aqueous coagulation bath. Circular, homogenous fibres were formed, which were carbonised at 1000 °C, with carbon fibre yields of up to 37%. The proof-of-concept monofilament carbon fibres (452 MPa tensile strength and 43 GPa tensile modulus) outperformed carbon fibres generated from pre-isolated ionosolv eucalyptus lignin using the same fibre spinning approach. A techno-economic analysis (TEA) of the modelled process at scale suggests that carbon fibre production costs were $9.02 kg^{-1} for the integrated process and $9.69 kg^{-1} for the redissolution-spun carbon fibres, while life cycle assessment (LCA) indicated that 20.7 kg CO_2-eq and 25.3 kg CO_2-eq greenhouse gas emissions were associated with integrated and redissolution spinning, respectively, providing strong motivation for future optimisation of the carbon fibres' mechanical performance and for process development.

Sustainability spotlight

Carbon fibre-reinforced plastics are strong, lightweight materials that replace steel, aluminium and glass fibre composites. While the composites are energy-efficient during use, carbon fibre production is reliant on fossil raw materials, employs toxic chemicals, such as acrylonitrile and hydrogen cyanide, and is highly energy-intensive. Carbon fibre composites are also expensive, limiting deployment and hence societal benefits. This study showcases the integration of two promising biorefining approaches with the goal of reducing reliance on fossil raw materials and improving the sustainability of carbon fibre production. Experimental data are accompanied by a rigorous life cycle assessment and a technoeconomic model to highlight the potential for reducing global warming impact and carbon fibre production costs. The new methodology promotes progress on various UN Sustainability Development Goals, including "Decent work and economic growth" (SDG 8), by developing a processe that is simpler and uses fewer hazardous chemicals and "Industry, innovation and infrastructure" (SDG 9) by developing a production method that reduces greenhouse gas emissions and supports the use of renewable feedstocks.

Introduction

Carbon fibre is a critical reinforcement for lightweight structural materials, particularly for polymer matrix composites used in aerospace, wind turbine and automotive construction. Conventional carbon fibres are produced through the pyrolysis of petroleum-derived precursor fibres. Significant costs are associated with precursor fibre formation (~50% of the total cost).[1] The petroleum-based precursors, mostly polyacrylonitrile (PAN), provide excellent mechanical performance (3–7 GPa tensile strength and 200–600 GPa tensile modulus) but require extraction of fossil resources and the use of expensive solvents such as dimethylformamide or dimethyl sulfoxide and are linked to the handling of highly toxic chemicals, in particular acrylonitrile and hydrogen cyanide.[2] PAN can be generated from biobased acrylonitrile;[3] however, even once developed to a commercial scale, biobased PAN carbon fibres can be expected

[a]*Department of Chemistry, Imperial College London, W12 0BZ, UK. E-mail: agi@imperial.ac.uk*

[b]*Department of Chemical Engineering, Imperial College London, SW7 2AZ, UK*

[c]*Department of Materials, Imperial College London, SW7 2AZ, UK*

[d]*Centre for Neural Circuits and Behaviour, University of Oxford, OX1 3SR, UK*

† Electronic supplementary information (ESI) available. See DOI: https://doi.org/10.1039/d5su00218d

‡ These authors contributed equally to the work.

to cost at least as much as conventional PAN. At the same time, sustainability benefits may be limited given the proposed multi-step syntheses, motivating the continued search for sustainable low-cost precursors from biopolymers.

Lignin is one of the most abundant biopolymers on Earth and is extracted from wood (lignocellulosic biomass) at the multi-million-tonne scale during paper and board production.[4,5] Most of the extracted lignin is currently incinerated to generate process energy and electricity. It is projected that less than half of the extracted lignin is needed to supply thermal energy in emerging lignocellulosic biorefineries,[6] leaving vast quantities to be used as raw material for carbon-containing chemicals and materials. Since many extracted lignins are mixtures of macromolecules with a substantial proportion of non-hydrolysable linkages,[7] the conversion to small molecules such as benzene derivatives is challenging.[8] Applications that utilise extracted lignin in the macromolecular form are therefore desirable. Lignin pyrolysis can result in relatively high carbon yields (typically 30–50%), approaching the carbon yield obtained from PAN (∼55%), while the lignin carbon fibre yield is significantly higher than that from cellulose precursor fibres (∼10–20%); hence, the production of lignin-derived carbon materials has attracted considerable interest.[1,2,9–11] However, lignin-derived carbon fibres are not commercially available due to a lack of industrially developed fibre production methods. Reported mechanical properties vary, with state-of-the-art performance for optimally processed lignin carbon fibres derived from precursor fibres with >50% biobased content reported to reach tensile strengths and moduli in the ranges 1–1.4 GPa and 70–100 GPa, respectively,[12–14] although exceptional tensile strengths (>2 GPa) and moduli (>100 GPa) have been reported recently.[15,16]

Fibres with high lignin content can be formed through melt spinning, either pure[16] or in blends,[15,17] which does not require a solvent. Dry spinning[12,18,19] generates lignin fibres after dissolution in volatile solvents, for example, water, acetic acid or ethanol–water mixtures, which are evaporated during fibre formation. Both approaches typically require purification,[20] fractionation,[12,18,21] or chemical modification[22–24] before spinning, adding cost and environmental burdens. Long, uneconomical stabilisation times for melt-spun lignin fibres have also been reported.[20,25] Fibres can also be formed through wet or coagulation spinning of lignin dissolved in a solvent (the dope) and spun into a coagulation bath containing a second solvent with negligible lignin solubility. Wet spinning is the general approach used for manufacturing PAN precursors.[2] Industrial, unfractionated lignins can be transformed into fibres using wet-spinning, but typically rely either on the same solvents used in PAN fibre spinning[26] or on more expensive alternatives.[13] Due to its low molecular weight, lignin requires a fibre-forming polymer additive for successful wet-spinning. Established examples include poly(ethylene oxide) (PEO),[27] cellulose,[13] PVA,[26] or PAN,[28] which are commercial polymers but 2–3 times more costly than technical lignins. Hence, there is a need to identify inexpensive and recyclable solvents for wet spinning lignin that minimise the quantity of spinning additive required.

ILs have been studied as solvents for dissolving hydroxylated macromolecules including the biopolymers cellulose, hemicellulose and lignin.[29] As part of this effort, a family of easy-to-prepare protic ionic liquids was identified as recyclable media for extracting lignin and hemicellulose from wood to obtain cellulose pulp,[30] generating a solution from which lignin is precipitated by increasing the water content (antisolvent precipitation).[31] Alkylammonium hydrogen sulfate–water mixtures have been identified as cost-effective media for ionosolv fractionation[32,33] and shown to fractionate a wide range of wood types.[34–37] ILs have also been used for the wet-spinning of cellulose and cellulose–lignin precursor fibres into water; however, the ILs 1-ethyl-3-methylimidazolium acetate, [Emim][OAc],[13] and 1,5-diazabicyclo[4.3.0]non-5-ene acetate, [DBNH][OAc],[38] are expensive ($25–35 kg^{-1})[39] and require near-complete drying to achieve acceptable polymer loadings in the dopes. Recently, we developed a novel lignin spinning method using aqueous mixtures of the ionosolv ionic liquid N,N-dimethylbutylammonium hydrogen sulfate, [DMBA][HSO$_4$],[40] which can be produced for <$1 kg^{-1} at an industrial scale,[39] 3–5 times lower than the bulk cost of DMSO. We showed that a dope solvent consisting of [DMBA][HSO$_4$] and 40% water enables the spinning of lignin fibres with up to 90% lignin content using only water as the coagulant. The fibre-forming additive was partially hydrolysed PVA, a biodegradable[41] and potentially biobased industrial polymer. Carbonised fibres with good carbon yield (up to 42%) were prepared from a range of lignins, including lignin obtained from industrial pulp mills. The approach uses low-cost and benign raw materials, such as unmodified lignin, PVA and water, in addition to the non-flammable ionic liquid–water mixture. Limited information is available on the health hazards of the ionic liquid; however, residual IL left on the cellulose pulp has been shown to be non-toxic in anaerobic digestion and insect feeding.[42] It is an acid–base complex of sulfuric acid and the trialkylamine, so its health hazards likely include moderate acidity and dermal toxicity associated with the N,N-dimethylbutylamine. The solvent is non-flammable and unlikely to be persistent and accumulative in the environment, given its constituents. The hazards need to be managed at a potential production site, which should be feasible for carbon fibre manufacturers, who are used to handling teratogenic and toxic dimethylformamide (DMF) and dimethylacetamide (DMAc) solvents.

Since [DMBA][HSO$_4$]–water mixtures have been effective for wet-spinning lignin fibres and for extracting lignin from wood biomass, we hypothesised that the two technologies could be combined to create an overall more efficient route ("integrated spinning") which uses the lignin-rich extract (black liquor) from ionosolv fractionation as a precursor for the spinning dope, avoiding isolation of the lignin (Fig. 1). Here, we test this new idea and evaluate the potential savings associated with process simplification. Eucalyptus wood was selected as the raw material for this proof-of-concept study for three reasons: it has a high lignin content,[36] has shown excellent spinnability in our previous study,[40] and is a fast-growing, commercially relevant hardwood species, providing feedstock for ∼40% of the chemical cellulose pulp market in 2021.[43] The extracted eucalyptus
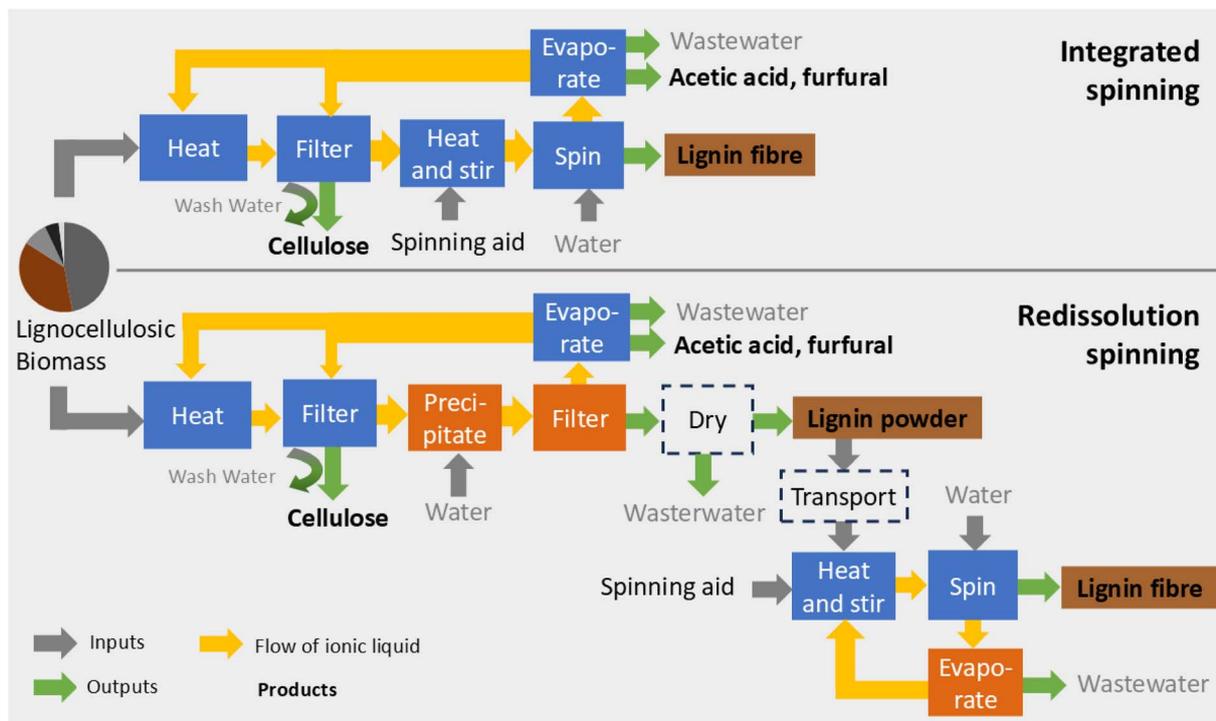
Fig. 1 The process for generating ionosolv lignin precursor fibres employing lignin extraction and fibre spinning separately (redissolution spinning) and the integrated spinning method demonstrated in this study.

ionosolv lignin is expected to be a depolymerised hardwood lignin, with a molar weight (Mw) of around 3000–4000 g mol^{-1} and a dispersity of 3–4.[36] However, the method is expected to generalise to a wider range of lignocellulosic biomass types, as both ionosolv extraction and fibre spinning have shown feedstock flexibility. In addition to the technical proof-of-concept, we have explored the cost and environmental impact of lignin-derived carbon fibre production using prospective technoeconomic (TEA) and life cycle assessment (LCA) analysis to evaluate whether further development of the integrated method is warranted.

Experimental

Materials

Eucalyptus wood (*Eucalyptus grandis*, also Red Grandis) was purchased from W. L. West & Sons Ltd, UK. The eucalyptus wood was milled to a particle size below 1 cm with a cutting mill (Retsch SM 2000) and stored in a plastic bag away from sunlight. The moisture content of the biomass was determined in triplicate by measuring the loss of mass during drying at 105 °C for at least 24 h according to a protocol published by the National Renewable Energy Laboratory (NREL).[44] Partially hydrolysed poly(vinyl alcohol) (PVA) was purchased from Kuraray Poval (No. 13-88, 88% hydrolysed, Mw 100 000 g mol^{-1}) and used as received. The ionic liquid [DMBA][HSO$_4$] with an acid-to-base ratio of 1 : 1 was synthesised from N,N-dimethylbutylamine and sulfuric acid with known water content in a custom-built flow reactor, as described previously.[40]

Ionosolv lignin extraction

The ionosolv black liquors were generated following the ionoSolv fractionation procedure at a scale of 9 g and 12 g eucalyptus wood with 30 g [DMBA][HSO$_4$] (water content 17 wt%) in triplicate at 150 °C for 1 h.[45] Water for lignin precipitation was not added as usual; instead, the ethanol and water were evaporated to obtain reconcentrated black liquor 30 and black liquor 40, referring to the biomass (over-dried basis) to solvent ratio. Details are provided in the (ESI) file.†

Determining the lignin loading in the black liquor

The quantity of lignin in the black liquor ("lignin fraction") was estimated by assuming that the lignin that was not found in the cellulose pulp was present in the ionic liquid solution and available to participate in fibre formation. Lignin content in the eucalyptus wood and the cellulose pulps was determined by compositional analysis according to a standard published procedure by the US National Renewable Energy Laboratory (NREL).[46] Details of the calculations used to determine the lignin fraction or lignin to solvent ratio can be found in the ESI.†

Determining the water and ethanol content in the black liquor

The water content (in wt%) in the black liquor was determined with a C20 coulometric Karl-Fischer titrator (Mettler Toledo) once per liquor replicate, and the average was recorded. The weight ratio (in %) of ionic liquid to ethanol in the liquor was determined using ^{1}H-NMR spectroscopy. The ^{1}H-NMR spectra and the calculations to determine the weight ratio can be found in the ESI.†

Preparation of the spinning dope

To prepare the spinning dope, the procedures published by Yang et al.[40] were followed with modifications. An aqueous PVA solution was prepared according to the formulae presented in the ESI.† A spreadsheet for calculating the input quantities is provided in the data repository. A part of the aqueous PVA solution was mixed with black liquor at 60 °C while stirring at 700 rpm for 1 h or 6 h in a 10 mL round bottom flask with a stir bar before being loaded into a syringe for fibre spinning.

The water content in the dope was fixed at 20% in all dopes instead of 40% due to the presence of residual ethanol after black liquor reconcentration. The polymer-to-liquid ratio was determined by the lignin fraction in the liquor, while the lignin–PVA ratio was adjusted via the PVA-to-water ratio in the aqueous PVA stock solution.

Examples: to prepare a dope with a target lignin to PVA ratio of 75 : 25 (3 : 1) and 20 wt% water fraction in the dope for liquor 40, 1.00 g of reconcentrated black liquor was combined with 0.284 g of an aqueous PVA stock solution with a 0.132 PVA-to-water ratio (by weight). To prepare a dope from liquor 40 with a target lignin to PVA weight ratio of 82.5 : 17.5 (4.71 : 1) and 20 wt% water fraction, 1.00 g of reconcentrated black liquor was combined with 0.272 g of a solution with a 0.0848 PVA-to-water ratio. Details of the calculations to determine the PVA loading in the PVA aqueous stock solution and the derivation of the equations are provided in the ESI.†

Viscosity measurements

The shear viscosity of the spinning dopes was measured using an AR 2000ex rheometer with a cone-and-plate fixture (2° cone angle, 20 mm plate diameter and 53 μm gap) at shear rates of 1 to 1000 s^{-1} at room temperature. Samples were conditioned by pre-shearing at 1 s^{-1} for 1 min, then held for a 2 min equilibration before performing the steady-state flow measurements. Each measurement was held for 30 s.

Fibre spinning

Fibre spinning followed the same procedure and method as described by Yang et al.[40] The dope solution was aspirated into a 1 mL plastic syringe and air was carefully expelled. The dope solution (ca. 0.5 mL) was extruded at room temperature with a syringe pump (KDS LEGATO(TM) 100, KD Scientific, US) at an extrusion rate of 1.5 mL h^{-1}. The coagulation bath was a Petri dish containing deionised water as the coagulant which was placed on a rotational table at 3.5 rpm. Custom-made Z-shaped cannula needles (Central Surgical UK) with a needle gauge of 29 (29 G, internal diameter 184 μm) were used as the spinneret. The bath was rotated at ca. 3 cm s^{-1} at the point of injection (8.3 cm from the centre) to provide extensional flow during fibre coagulation. The ratio of rotation speed at the point of injection to the injection speed was 2.5. The fibres were coagulated for 2 min in a water bath and picked up using tweezers. Fibres spun from dopes with a 75 : 25 lignin to PVA ratio were hung on a rod under tension from a known weight (i.e., a piece of aluminium foil) that was attached to the bottom end of the fibres (50 mg, ~0.5 mN) and fibres spun from dopes with an 82.5 : 17.5 lignin to PVA ratio were hung under ~0–0.1 mN tension. Fibres were air-dried overnight.

Oxidative stabilisation and carbonisation of lignin PVA fibres

The lignin–PVA precursor fibres were hung vertically under tension of a small weight (ca. 0.5 mN) and stabilised in air in a convection oven (Memmert UNP-200) by heating from 25 to 100 °C at 1 °C min^{-1} and from 100 to 250 °C at 0.2 °C min^{-1}, followed by holding at 250 °C for 1 h. 10 cm long sections of stabilised fibres were fixed onto a graphite bridge using RESBOND™ 989 ceramic adhesive and carbonised in a quartz tube furnace (OTF-1200X-III-S-NT) under N$_2$ flow (50 mL min^{-1}) using a heating ramp from 25 to 1000 °C at 1 °C min^{-1} followed by a hold at 1000 °C for 2 h.

Coagulated fibre yield

0.270 g of poly(vinyl alcohol) (Kuraray Poval, 88% hydrolysed, 100 000 g mol^{-1}) was added to 1.778 g of deionised water and stirred at room temperature for 15 min, then at 85 °C for 45 min until complete dissolution was observed under an optical microscope. 0.989 g of the aqueous poly(vinyl alcohol) stock solution was added to 3.654 g of black liquor 40 to generate a 75 : 25 lignin to PVA ratio and stirred at 60 °C for 6 h. The dope solution was extruded through a 27 G Z-shaped cannula at an extrusion rate of 1.5 mL h^{-1} into deionised water. The fibres were extruded at a radius of 7 cm and left in a water bath for 2 min before extracting the entire fibre coil from the bath with tweezers. The fibre coil was set on a square of pre-weighed aluminium foil (0.15 g) and left to air dry overnight. The aluminium foil with the air-dried fibres was folded into a parcel and placed in a Thermo Scientific Heratherm oven for 24 h at 105 °C, and the subsequent mass of each parcel was recorded. The yield was calculated by dividing the oven-dried fibre weight by the amount of lignin and PVA present in the extruded volume of the dope. Five measurements were performed, and the average and standard error of the mean are presented.

Thermogravimetric analysis (estimated carbon yield)

The carbon fibre yield after carbonisation was estimated using a thermogravimetric analyser (Mettler Toledo TGA/DSC 1LF/UMX). The samples were heated in platinum pans at 10 °C min^{-1} under N$_2$ flow (50 mL min^{-1}) from 25 °C to 100 °C, held isothermally at 100 °C for 30 min to drive off moisture followed by increasing the temperature to 900 °C at 10 °C min^{-1}. Blank runs were conducted for each sample using empty platinum pans to obtain baselines for correcting the buoyancy effect. These baselines were subtracted from experimental runs and weight values were normalised to 100% at the start of the second ramp. For each sample, TGA measurements were carried out in at least duplicate, and the average values of the carbonisation yields at 900 °C were recorded.

Optical microscopy

Optical microscope images of the dope were collected on a Leica DM2500 microscope with a Basler Ace acA1920 camera. The sample was prepared by drawing the solution into a syringe through a needle from the dope, followed by depositing a small drop on a glass slide from the needle. The sample was covered with a cover slide and imaged. Crossed polarisers were used to identify birefringent particles. Fibre diameters were measured at a magnification of $10\times$ using the Automatic White Balance mode.

Scanning electron microscopy (SEM)

SEM images of the air-dried lignin–PVA fibres were recorded on a JEOL JSM-6010LA microscope using Secondary Electron Imaging (SEI) (Everhart-Thornley detector) with a working distance of 15–20 mm and a 20 kV accelerating voltage. The fibres were broken into pieces with tweezers and mounted on an aluminium stub using carbon adhesive tape. Precursor fibre samples were sputter-coated with chromium before imaging. Carbonised fibre samples were imaged using the same instrument settings but without coating.

Tensile testing

The tensile strength and stiffness of the lignin–PVA precursor fibres and carbonised fibre samples were determined using the standard test method ISO BSI11566. The single filaments were mounted on a card template (15 mm gauge) using an epoxy adhesive (Araldite Rapid, Huntsman Corporation, US). Samples were tested using a tensile tester (TST350, Linkam Scientific Ltd GB) fitted with a 20 N loading cell at 16.7 μm s^{-1} until failure. The tensile modulus was determined from linear regions between 0.2% and 0.5% strain. The cross-sectional areas of the samples were measured using an optical microscope.

Raman spectroscopy

A Renishaw inVia micro-Raman spectrometer with a $50\times$ magnification lens and a 50 mW 532 nm laser operated at a laser power of 5% and an exposure time of 2 s with 5 acquisitions was used for the acquisition of Raman spectra. The spectral range was 800–3200 cm^{-1} and spectra were averaged over five different locations along the carbon fibre surface. The intensity ratio of the D-band (1350 cm^{-1}) to the G-band (1590 cm^{-1}), I_D/I_G, was measured after fitting the bands with a Lorentzian function using WiRE 4.1 software.

Technoeconomic and sustainability evaluation

Details of the TEA and LCA can be found in the ESI.† The LCA was carried out according to the ISO 14040-14044 standard following the four key interactive stages,[47] including goal and scope definition, life cycle inventory, life cycle impact assessment and interpretation. A functional unit of 1 kg lignin-based carbon was used. The boundary of assessment was defined from cradle-to-gate starting from the feed biomass source (eucalyptus wood chips) and comprising biomass pre-processing (crushing, drying and milling), ionosolv fractionation to produce the lignin precursor and the carbon fibre manufacturing stages ("carbonisation").

Results

Process concept

During ionosolv fractionation of lignocellulosic biomass (here eucalyptus wood), the majority or all of the hemicellulose and the majority of lignin are extracted into an ionic liquid–water mixture (Fig. 1). The acetylated hemicellulose, mostly composed of xylan (Table S1†) is depolymerised during the extraction, generating soluble acetic acid, furfural, saccharides and water-insoluble humins over time.[33] The lignin-containing black liquor is mixed with water, which causes the lignin to precipitate, as water is a non-solvent for lignin. The precipitated lignin is washed and dried to isolate powdered lignin for subsequent use, while the ionic liquid can be concentrated in an evaporator and reused. The evaporation also enables isolation of volatile dissolved co-products.

For fibre spinning, this powder is redissolved in the ionic liquid–water mixture along with the spinning aid (PVA) to make a spinning dope with $\sim$14 wt% polymer loading (PVA + lignin) which is spun into water and called "redissolution spinning". To create an integrated spinning process ("integrated spinning"), the ionosolv black liquor must be converted into a spinning dope by adding the spinning aid without lignin isolation. The lignin content in the liquor must be high to achieve a spinnable dope composition which can be achieved by using a high biomass loading during ionosolv fractionation. The biomass loading applied in this work was, therefore, higher than in standard ionosolv fractionation experiments (typically 2 : 10); however, ionosolv fractionation has previously been shown to effectively extract most lignins at up to a 1 : 1 biomass to solvent ratio.[35,48] To match the polymer loadings used for previous redissolution spinning experiments, biomass-to-solvent ratios of 3 : 10 (30 wt% biomass loading, black liquor 30) and 4 : 10 (40 wt% loading, black liquor 40) were employed, with theoretical maximum lignin contents in the black liquor of 11% and 15%, respectively.

Lignin extraction and liquor composition

The ionosolv eucalyptus black liquors were generated by heating eucalyptus wood in [DMBA][HSO$_4$] containing 20% water at 150 °C for 1 h, an established fractionation condition shown to be suitable for many lignocellulose types.[35,36,49] In the laboratory, ethanol was used as a diluent to support the separation of the lignin-containing ionic liquid–water mixtures from the cellulose pulps; however, the industrial version of this process may obtain the black liquor by using recycled ionic liquid as wash solvent.[50] Lignin extraction was successful, generating cellulose pulps with yields of 45.6 $\pm$ 2.3% and 51.0 $\pm$ 0.5%, implying that 80.0 $\pm$ 2.1% and 72.5 $\pm$ 0.5% of the lignin was extracted for the 30% and 40% biomass loading experiments, respectively (Tables S1 and S2†). The delignification was lower than that reported in a previous study (92 $\pm$ 3%) using 20% eucalyptus wood loading and a similar ionosolv solvent.[33] The reduced efficiency can be attributed to the higher biomass-to-

Table 1 Polymer weight fractions and ratios in spinning dopes. The dopes were prepared from ionosolv black liquor 30 and black liquor 40. Polymer-to-solvent ratios for redissolution spinning (RS) have been converted to weight fractions for better comparison

Dope sample	Lignin to PVA ratio	Lignin fraction (%)	PVA fraction (%)	Polymer fraction (%)
75% dope 30	75 : 25	6.8	2.3	9.1
75% dope 40	75 : 25	7.8	2.6	10.4
82.5% dope 40	82.5 : 17.5	7.9	1.7	9.6
RS dope 75% (ref. 40)	75 : 25	10.3	3.5	13.8
RS dope 82.5% (ref. 40)	82.5 : 17.5	11.4	2.4	13.8

solvent ratio, leading to more extracted lignin reprecipitating onto the cellulose during ethanol washing (lignin has lower solubility in ethanol than in IL–water mixtures).

Dope preparation

To prepare the black liquor spinning dopes, the wash ethanol (EOH) was evaporated. Most of the water was also removed during the evaporation, as the reconcentrated black liquors contained less than 1 wt% water (Table S3†); the low water content is likely due to the low-boiling ethanol–water azeotrope (78.2 °C at atmospheric pressure). However, ^{1}H-NMR spectroscopy (Fig. S1†) indicated that ethanol from the cellulose pulp washing remained in the reconcentrated black liquor. The measured molar IL-to-ethanol ratios of 1.4 : 1 and 1.9 : 1 translate to estimated dope solvent compositions of 85 : 14 : 1 and 88 : 11 : 1 wt% fraction (IL : ethanol : water) for black liquor 30 and black liquor 40, respectively. Although not measured, other solutes generated during eucalyptus wood fractionation were present, including mono and oligosaccharides, furfural, HMF, and acetic acid, which originate from glucan and hemicellulose depolymerisation and conversion.[33] Based on the combined glucan and xylan removal from the original biomass, the amount of non-lignin solutes in the black liquor is estimated to be around half of the amount of dissolved lignin.

Optical microscopy of the black liquors (Fig. S2–S5†) showed that they were essentially homogenous solutions with few small (<10 μm) birefringent particles present, likely cellulose crystals that passed through the filter. The particles were significantly smaller than the spinneret diameter and hence not expected to affect fibre coagulation significantly. The reconcentrated black

liquors were used to prepare the spinning dope by adding PVA as a spinning aid. Since the PVA flakes did not dissolve directly in the black liquor samples, the polymer was added as a solution, pre-dissolved in deionised water.

Fibre spinning

Dope 30 (prepared from black liquor 30) and Dope 40 (from black liquor 40) with the compositions shown in Table 1 were used to spin fibres into a coagulation bath containing deionised water. Despite the lignin fractions in the dopes being lower than used for redissolution spinning, fibres successfully formed from all dopes when using a 3 : 1 lignin-to-PVA ratio. The successful fibre spinning confirmed that neither the non-lignin solutes generated during wood fractionation, nor the residual wash ethanol introduced through the pulp-washing step hindered fibre formation. Increasing the dope preparation time from 1 h to 6 h increased the dope viscosity and the resulting fibre diameter (Table 2).

Ideally, the lignin content of the fibres should be maximised to increase the carbon fibre yield and reduce carbon fibre cost.[1] However, dopes with the higher lignin-to-PVA ratio (82.5 : 17.5%) were difficult to spin, presumably due to the low PVA content in the dope, resulting in a low dope viscosity (Fig. S6 in the ESI†). A longer dope preparation time (6 h) resulted in a viscosity increase of 25% (Fig. S6b†), which was sufficient to spin continuous lignin–PVA fibres from Dope 40.

Characterisation of lignin–PVA fibres

SEM imaging (Fig. 2 and S8†) confirmed that the air-dried lignin–PVA fibres had uniform diameters and circular cross-sections

Table 2 Diameter, tensile properties, and estimated carbon yield (by TGA) for air-dried eucalyptus lignin PVA fibres prepared from integrated and redissolution spinning dopes

| Biomass loading (%)	Dope preparation time (h)	Lignin to PVA ratio	Needle I.D. (μm)	Fibre diameter (μm)	Tensile strength (MPa)	Young's modulus (GPa)	Strain at break (%)	Est. carbon yield (%)
30	1	75 : 25	184	59.2 ± 3.6	43.6 ± 2.4	4.7 ± 0.1	1.0 ± 0.0	29.1 ± 2.6
30	6	75 : 25	184	78.1 ± 3.4	47.5 ± 1.8	5.0 ± 0.3	1.0 ± 0.1	30.6 ± 0.6
40	1	75 : 25	184	86.0 ± 1.5	43.4 ± 1.8	4.8 ± 0.1	1.0 ± 0.1	32.2 ± 0.5
40	6	75 : 25	184	93.2 ± 5.0	40.6 ± 2.3	4.8 ± 0.4	0.9 ± 0.1	35.7 ± 0.2
40	6	82.5 : 17.5	184	75.3 ± 5.3	39.1 ± 7.8	4.8 ± 0.7	0.9 ± 0.1	36.6 ± 1.1
From lignin powder[40]	1	75 : 25	210	123.4 ± 11.7	30.0 ± 1.9	2.8 ± 0.1	1.2 ± 0.1	40.7 ± 1.2
From lignin powder[40]	1	82.5 : 17.5	210	128.6 ± 2.8	21.2 ± 2.3	4.3 ± 0.1	0.5 ± 0.1	42.2[a]

[a] Single measurement.
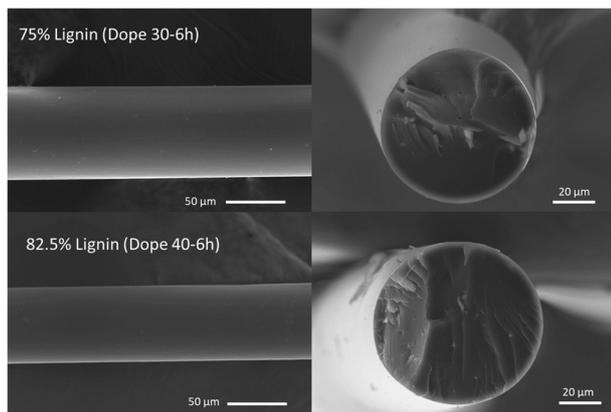
Fig. 2 SEM images of lignin PVA fibres prepared from 30% and 40% ionosolv black liquors using 6 h preparation time and a 75 : 25 or 82.5 : 17.5 lignin-to-PVA ratio.

Fig. 3 Thermogravimetric analysis data of lignin PVA fibres generated through integrated spinning to estimate the carbon fibre yield.

regardless of polymer content and dope preparation time, which demonstrates a well-controlled coagulation process, similar to the spinning of isolated lignin and PVA dissolved in fresh IL–water mixtures.[40] Many other precursor wet-spinning processes (both for PAN and lignin) produce crenulated or kidney bean shaped cross-sections due to mass transport issues during coagulation; it is an attractive feature of the IL-water solvent that circular fibres are obtained even at relatively large diameters. The continuity of the IL-water dope composition with the water coagulation bath may help to balance the coagulation and diffusion rates; similarly, circular fibres were obtained previously using the (more expensive) ionic liquid [Emim][OAc].[13] Despite the well-formed cross-section, small pores were visible in some fibres, likely due to air bubbles in the dope solutions, which are associated with limiting fibre mechanical properties. Such pores could be reduced by degassing the dope more thoroughly. The fibre diameters (53–93 μm) were smaller than those of fibres obtained from dissolved eucalyptus ionosolv lignin (120–130 μm) under similar spinning conditions, which correlates with the lower dope viscosities (Fig. S6†). Dopes with a higher viscosity formed gel protofibres with larger diameters due to less extensional drawing experienced in the rotational coagulation bath. Other factors also play a role, as can be seen in Fig. S7,† including the spinneret (needle) diameter and the polymer loading in the dope.

Comparison of the collected precursor fibre mass and the nominal solid content injected during spinning (for Dope 40 with a 75 : 25 lignin to PVA ratio and 6 h dope preparation time) indicated that 9.6 wt% of polymer weight was lost to the coagulation bath during spinning (Table S6†). The more soluble (*aka* "acid-soluble") lignin may be lost preferentially. It is hence likely that the lignin-to-PVA ratio in the precursor fibres was lower than intended.

The air-dried lignin–PVA fibres generated from various compositions had similar tensile strengths (39–48 MPa), moduli (4.2–5.2 GPa) and strains at break (0.9–1.0%) (Table 2). The tensile strengths were similar to those of fibres prepared from isolated eucalyptus ionosolv lignin, but slightly higher overall. The tensile strengths of the lignin–PVA fibres were also similar to
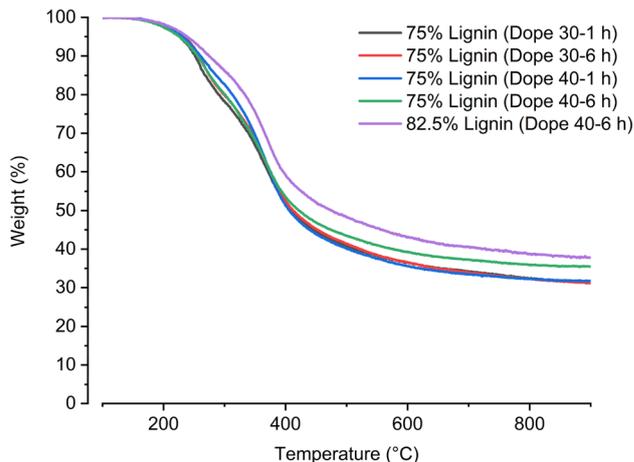
those reported for other spinning methods employing isolated lignins and PVA,[26] showing that integrating fibre spinning with lignin extraction does not negatively affect precursor fibre properties. The absolute values could likely be improved significantly at an increased scale, as discussed below.

Estimated carbon yield

The carbonisation process can be simulated on a small scale by thermogravimetric analysis (TGA) in a nitrogen atmosphere (Fig. 3 and Table 2). During industrial PAN-based carbon fibre production, precursor fibres are thermally stabilised in air before carbonisation to prevent fibre fusion at the pyrolysis stage; a separate stabilisation step was omitted in this TGA experiment to facilitate data acquisition. It is not clear whether stabilisation in air is relevant for lignin precursors, although it is often applied, likely due to experience with PAN. Recent work suggests that a small increase in yield may be obtained using air stabilisation compared to nitrogen stabilisation.[51]

TGA-measured carbon yields were in the 30–37% range, with higher yields obtained for dopes with higher lignin loading and longer dope preparation times. Longer dope preparation is thought to promote intermolecular interactions between PVA polymer chains and between PVA and lignin, as evidenced by increased dope viscosity. These interactions may help retain more lignin during coagulation and more carbon during pyrolysis. The estimated carbon yields for directly spun lignin fibres (29–37%) were lower than the yields observed for PVA–lignin fibres generated from isolated ionosolv eucalyptus lignin (41% and 42% for the 75 : 25 and 82.5 : 17.5 lignin to PVA ratios, respectively) and pure eucalyptus lignin (~44%).[40] The lower carbon yield may also be due to lower lignin-to-PVA ratios in the fibres than in the dope; however, more work is needed to understand the phenomenon and maximise carbon fibre yield. The reported carbon yields are comparable with those reported for wet-spun fibres using redissolved Kraft softwood lignin with cellulose or PVA as spinning aids (30–37% estimated or actual carbon yield).[13,26]
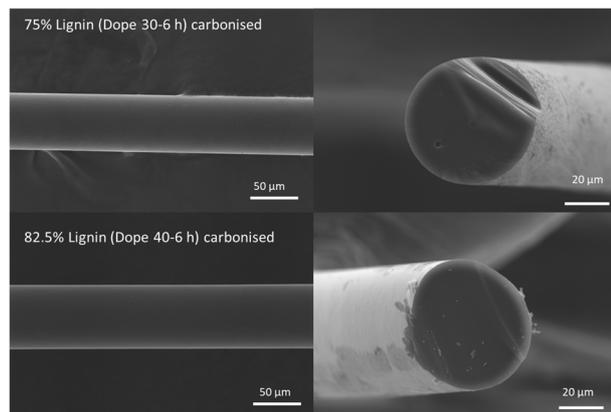
Fig. 4 SEM images of carbonised lignin PVA fibres generated by integrated spinning. Fibres were prepared from spinning dopes from black liquor 30 and black liquor 40 that were mixed with a PVA stock solution for 6 h.

Thermal conversion and carbon fibre characteristics

The lignin–PVA fibres were thermally stabilised in air at 250 °C followed by carbonisation at 1000 °C in nitrogen (with a heating rate of 1 °C min^{-1}). SEM images of the carbonised fibres (Fig. 4 and S9†) show that the round cross-sections and the smooth surfaces of the fibres were retained during carbonisation regardless of dope preparation conditions. It was observed that more pores were present on cross-sections and surfaces after carbonisation, likely due to the evolution of gases such as CO_2, CO and H_2O.

The fibre diameters were relatively large (51–63 μm, Table 3), which is typically associated with increased defect size, lower tensile strength and a reduced contribution from an ordered fibre skin. The carbonised fibres had tensile strengths of 300–450 MPa (Table 3), with no significant variation observed among the different samples. Interestingly, the measured strengths are higher than those obtained for carbonised eucalyptus PVA fibres generated *via* redissolution (RS) spinning in our previous study.[40] The cause of the increased tensile strength is unclear, although it may be due to the avoidance of defects associated with incomplete redissolution. The carbonised fibres' modulus was 35–43 GPa, similar to that of the carbonised fibres prepared from isolated lignin in our previous study. To ascertain the role of defects, the Weibull strength and modulus could be

calculated in the future.[19] These tensile properties did not reach the benchmark values for carbon fibres in automotive applications (1.72 GPa strength and 172 GPa tensile modulus)[1] or the state-of-the-art tensile properties for lignin fibres (~1–2 GPa strength and 100–260 GPa tensile modulus)[15] obtained at ~10 μm carbon fibre diameter, similar to those of commercial carbon fibres. However, the study's goal was to demonstrate a proof-of-concept of integrated spinning as a new process option. There are several standard engineering approaches to optimising fibre spinning, which should improve the fibre mechanical properties, such as the application of tension and fibre drawing. Applying continuous multifilament tow spinning will enable the reduction of fibre diameter.[15,16,19] Better filtration of the black liquor should remove cellulose fibre fragments which likely cause defects due to their lower carbon yield, while improved dope degassing will minimise void formation. The impact of impurities from either the biomass (ash, extractives, and protein) or the extraction process (ionic liquid) on the fibre should be explored systematically in the future. Precursor fibre drawing, optimising the temperature programme and tensioning during stabilisation and carbonisation could improve atomic alignment in the final carbon fibres. While some studies report their best mechanical properties at 1000 °C, others report best performance at 1200–1400 °C,[13,19] so carbonisation temperatures above 1000 °C could be explored.

Raman spectroscopy

Raman spectroscopy is well suited to studying the graphitic structure of carbon materials. The Raman spectra of the carbonised fibres show three prominent signals (Fig. 5): the defect-induced D band (~1350 cm^{-1}), the sp^2 carbon in-plane bond stretching mode G band (~1590 cm^{-1}) and a second-order signal 2D band with very low intensity (2400–3200 cm^{-1}). These signals prove the presence of a carbon structure; however, the broad D and G bands and the small 2D band suggest that the atoms are highly disordered, which is typical for lignin-derived carbons, particularly at a modest carbonisation temperature (1000 °C).[52] The intensity ratio of the D to G bands (I_D/I_G) provides semi-quantitative information about graphitic quality. In highly ordered graphite, I_D/I_G approaches 0 due to the absence of the defect-induced D band. Here, I_D/I_G was slightly above 1.0 (Fig. 5), similar to lignin–cellulose derived carbon fibres carbonised at the same temperature (1000 °C).[13] A higher temperature (~1200 °C)

Table 3 Diameter and tensile properties of the carbonised lignin PVA fibres derived from eucalyptus lignin spun through a 184 μm needle. Reference precursor fibres generated through redissolution spinning (RS) were spun using a wider needle (210 μm)

| Sample	Lignin: PVA (wt/wt%)	Biomass loading (%)	Dope preparation time (h)	Fibre diameter (μm)	Tensile strength (MPa)	Modulus (GPa)	Strain at break (%)
75% lignin (dope 30–6 h)	75 : 25	30	6	55 ± 3	312 ± 62	35 ± 1	1.0 ± 0.2
75% lignin (dope 40–1 h)	72 : 25	40	1	51 ± 3	444 ± 55	43 ± 1	1.2 ± 0.1
75% lignin (dope 40–6 h)	72 : 25	40	6	63 ± 6	367 ± 103	35 ± 2	1.2 ± 0.2
82.5% lignin (dope 40–6 h)	82.5 : 17.5	40	6	62 ± 4	435 ± 37	37 ± 2	1.0 ± 0.1
75% lignin (RS)[40]	72 : 25	N/A	1	77 ± 13	291 ± 37	40 ± 3	0.6 ± 0.1
82.5% lignin (RS)[40]	82.5 : 17.5	N/A	1	91 ± 5	282 ± 35	36 ± 2	0.9 ± 0.1
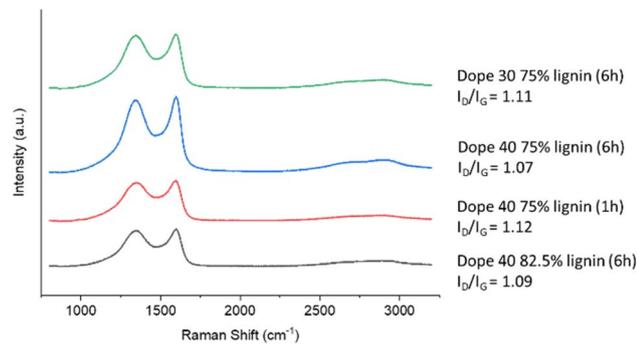
Fig. 5 Raman spectra of carbonised lignin PVA fibres obtained through integrated spinning.

might induce more graphitisation and improve mechanical properties, particularly the Young's modulus.[13]

Process model development

To understand the implications of integrating lignin extraction and carbon fibre spinning, we performed an LCA and cost analysis of the process and compared it to redissolution spinning. The analysis was carried out based on the process concepts shown in Fig. 1, with detailed process flows shown in Fig. S10 and S11 in the ESI.† The process was divided into six production stages to allocate impacts and costs: feed biomass, lignin extraction, lignin precipitation, dope formation, precursor fibre spinning, and carbonisation. The carbonisation stage includes precursor fibre stabilisation. The plant was designed to process 788 tonnes (~100 kg h^{-1}) of biomass per annum, the plant design life was assumed to be 25 years, and the interest rate was set to 10%. Our model captures all processes from the biorefinery gate, while upstream activities such as biomass production and power generation are quantified from databases.

The process inventory (Tables S7 and S8†) shows relevant parameters across the production stages for integrated and redissolution spinning, respectively. Assumptions for the model were based on data from this study and from the study by Yang *et al.*, with some modifications. For lignin extraction, the eucalyptus wood loading for both process options was assumed to be 40%, with an increased lignin extraction of 90%, with the composition presented in Table S1.† The increased lignin extraction is reasonable, as the high residual lignin content in the pulp is attributed to the use of ethanol as wash solvent in the lab-scale procedure, which would be omitted in the industrial process.[46] 51% of the biomass was assumed to become unbleached cellulose pulp while 11.2% was xylan that was converted to furfural and 4.8% was acetic acid, which are co-products of the process. The water content in the extraction solvent was 20% and the solvent recovery was assumed to be 99.5%, which is reasonable based on a recycling study for a similar ionic liquid.[32] The IL was reused 10 times for the base case (a sensitivity analysis for IL recycling is performed later). For redissolution spinning, the dilution ratio of the IL to precipitate the lignin was 4 : 1 and three washes were assumed for the cellulose.

For carbon fibre production, the lignin-to-PVA ratio in the dope solvent was 4 : 1, an estimated minor reduction from the lab scale process; the biomass loading was 40 wt% and the polymer fraction in the dope was 8% of the total mass in the redissolution spinning dope; the coagulated lignin PVA fibre yield was 100% for redissolution spinning and 90% for integrated spinning, based on the experimental data presented in this paper. Two further assumptions, subject to future verification are as follows: (a) the use of a coagulation bath with 20 wt% IL content rather than deionised water, applied to facilitate energy-efficient recovery of the dope solvent, and (b) that stabilisation can be achieved within 1 h at 250 °C in air, which is shorter than the experimental procedure used in this study, but is a reasonable assumption based on previous reports.[52] Carbonisation at 1000 °C in nitrogen gas was assumed to result in carbon fibre yields of 42.0% and 36.6% for redissolution and integrated spinning, respectively, based on experimental data from this and our previous study.[40] The energy source was the United Kingdom's 2024 grid electricity system, which comprises a combination of non-renewable and renewable energy sources. Emissions from the carbonisation were not evaluated, as there are no experimental data on the composition of the off gases for the ionosolv carbon fibre approaches or other proposed lignin carbon fibre methods. The off-gases from lignin carbonisation are not known but they are likely a range of compounds including CH_4, CO_2, CO, water and volatile tars and would require appropriate abatement methods.[53]

Sustainability evaluation of ionosolv lignin fibre spinning

In recent years, interest in evaluating the sustainability of high-value materials has grown,[54,55] including carbon fibre derived from renewable sources.[56–58] The interest is reflected in the rising demand for carbon fibre in various sectors, including aerospace, automotive, and energy.[58] Using fossil-derived alternatives for carbon fibre production requires thorough scrutiny and assessment to avoid unintended environmental consequences. Hence, a sustainability assessment was conducted to evaluate the environmental implications of lignin-based carbon fibre production *via* integrated spinning, compared to both redissolution spinning, as published by Yang *et al.*,[40] and standard modulus PAN-based carbon fibre. While lignin-based carbon fibres currently do not have the material performance of PAN-based carbon fibres, designers and engineers often have standard modulus PAN fibre in mind for sustainability and cost comparison, even if they do not expect to use all the properties. The analysis was conducted with 1 kg of carbon fibres as the functional unit for simplicity, despite differences in properties, since the relevant performance profile varies by application, and the ultimate mechanical properties of lignin-derived carbon fibres are unknown. Emissions savings from the co-products, acetic acid and furfural, were assigned to the fibre spinning unit. Cellulose is a valuable product and is sold on the market in this study, based on previous findings that ionosolv cellulose retains the native structure of wood cellulose.[30] The revenue and environmental credits for cellulose in this model are for an unbleached cellulose pulp product, excluding the energy and chemical requirement for downstream cellulose upgrading.
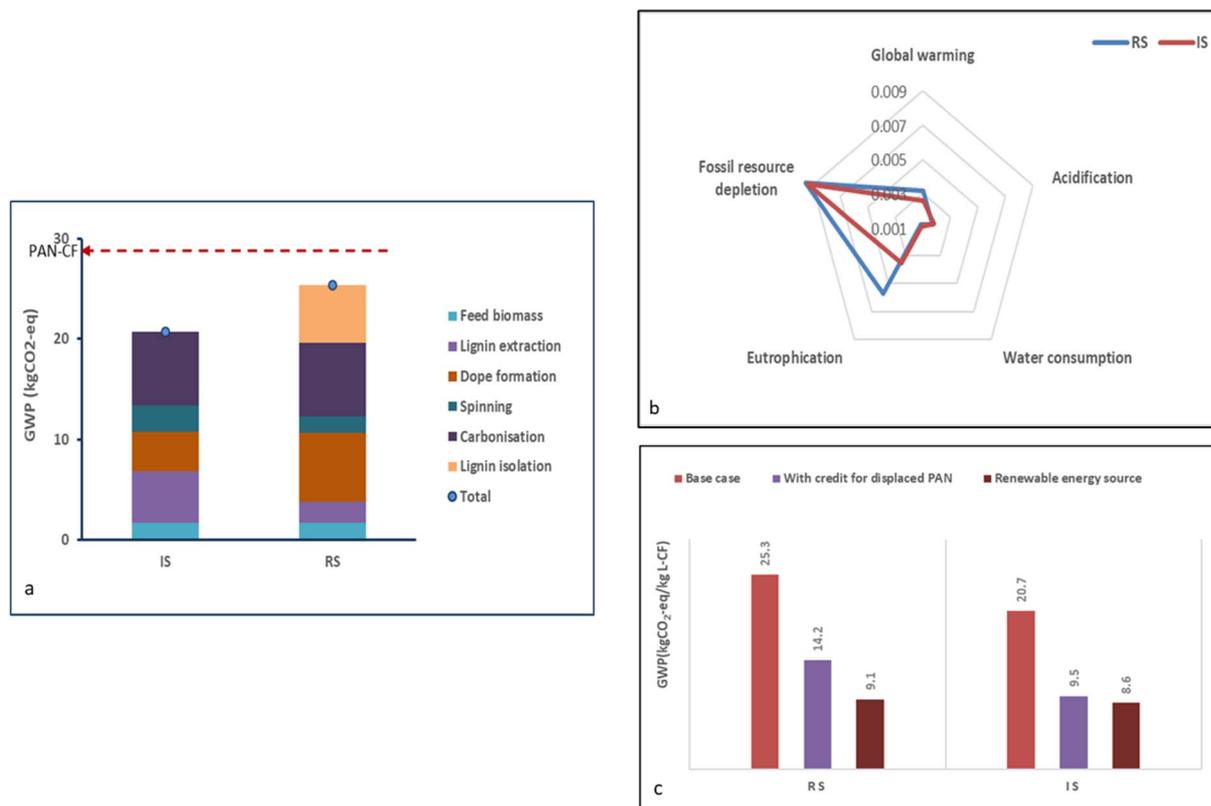
Fig. 6 Environmental impact of lignin carbon fibres generated through redissolution spinning (RS) and integrated spinning (IS). (a) Global warming potential broken down into production stages, benchmarked against an optimistic GWP for PAN carbon fibres. (b) Normalised impact scores for lignin carbon fibre production across a range of impact categories. (c) Comparative analysis of GWP (kg CO_2-eq) against the baseline scenario for lignin carbon fibre production.

Global warming potential

The main goal of employing lignin-based carbon fibres is the reduction of climate impact. Hence, the focus was placed on the global warming potential (GWP). Fig. 6(a) shows that the modelled GHG emissions were 20.7 and 25.3 kg CO_2-eq per kg carbon fibre for the integrated and redissolution approach, respectively. The lower GWP of the integrated spinning process is attributed to the reduced number of operational stages in the fibre manufacturing phase. A breakdown of contributions for the various production stages for the redissolution approach shows that carbonisation, dope formation and lignin isolation contribute significantly to the GWP impact (29, 27 and 23%, respectively). Lignin isolation with the precipitation and washing stages accounts for ~36% of the operational energy demand in carbon fibre production *via* redissolution spinning (Table S8†). The impact of this energy use is avoided by employing integrated spinning.

Furthermore, the benefit of recycling the ionic liquid was captured in the assessment (~10 times at 99.5% IL recovery per cycle for the base case), which reduced the GWP impact of the fractionation unit. Since the recycling rate of the ionic liquid can in principle be higher,[33] the sensitivity of recycling the ionic liquid is discussed in the sensitivity analysis section. The carbonisation stage includes the fibre stabilisation and fibre

pyrolysis, with the former modelled at 250 °C and the latter modelled at 1000 °C in line with the experimental part of the study.

The contribution of precursor fibre carbonisation to the overall GWP was larger than that of other carbon fibre production stages due to the high temperature required, which aligns with expectation and existing studies on PAN carbon fibre production.[59] Several factors have been identified as influencing the energy intensity of fibre carbonisation, including the furnace type/geometry, heat losses, heat recovery efficiency, and duration of carbonisation. A sensitivity analysis, exploring a range of residence times and varying levels of heat recovery and heat losses is presented in Fig. S14 of the ESI.† The model suggests that lower energy consumption is achieved when the residence time is limited to 30 minutes and a low heat loss coefficient is achieved for the furnace. However, stabilisation furnaces aer designed to be open, where fibres repeatedly enter and exit, making insulation challenging.

Other impact categories

While existing studies on the LCA of lignin carbon fibres have utilised energy demand and GWP,[10,57] the environmental impacts can also be considered across a wider range of impact categories using normalised scores in a radar plot (Fig. 6b). The additional categories used in this study, eutrophication, water

consumption, acidification and fossil resource depletion, are considered relevant to carbon fibre production that requires biomass feedstock and aqueous solvents. The integrated spinning process indicates better sustainability performance across all impact categories except acidification, which is broadly similar. Redissolution spinning had a significant contribution to fossil depletion, which is attributed to the higher (fossil) energy use, while the increased contribution to the freshwater eutrophication category is attributed to additional wastewater discharged from the lignin isolation unit. The water consumption impact category is attributed to secondary processes, including sulfuric acid production and ammonia production *via* steam reforming, which are needed for IL production. It should be noted that the water use impact of electricity generation from secondary processes is broadly similar; however, primary water consumption was higher for the redissolution process. The acidification impact can be traced to sulfur dioxide emissions and processes related to butene and dimethylamine production, which are also part of the IL production.

The GWP for both base-case lignin carbon fibre production models falls within the range predicted for lignin carbon fibre production technologies by other models (15 kg CO_2-eq to 25 kg CO_2-eq) and is lower than the GHG emissions estimated for PAN carbon fibre spinning (27 kg CO_2-eq to 41 kg CO_2-eq).[10] Exceptionally, a GWP impact of only 1.5 kg CO_2-eq was calculated for carbon fibres from Lignoboost Kraft lignin generated *via* melt spinning.[57] In this study, the environmental burdens of the pulping process were allocated according to the economic value of the wood pulping products rather than by mass, which means that most GWP burdens associated with the wood fractionation were allocated to cellulose. A larger proportion of fossil energy was replaced with renewable energy (the Swedish region had a strongly decarbonised electricity grid in 2022) and energy from the pulping stage was recycled for use in the lignin carbon fibre production, showing that deploying renewable energy and energy recycling are key to achieving carbon fibres with low global warming impact.

Sustainability scenario analysis

The comparative analysis of the GWP impact for three scenarios with credit allocations is shown in Fig. 6c. Burden or credit allocation adds specific environmental loads or benefits to a system's components or activities. Credit allocation assigns the benefits from co-products, by-products, or displaced products as avoided burdens. For example, the impact of producing a co-product is subtracted from the total production impact. Three additional scenarios were investigated: implementing carbon credit for displacing PAN (1), use of 100% renewable energy sources (2), and comparison with fossil carbon fibres (3).

The allocation of carbon credit for substituting PAN with bioderived precursors for carbon fibre production resulted in a significant reduction in environmental impact from 20.7 to 9.5 kg CO_2-eq and from 25.3 to 14.2 kg CO_2-eq for integrated and redissolution spinning, respectively. Replacing the UK grid electricity system with fully renewable electricity sources (*e.g.*, wind turbines) reduced the base case GWP to 8.6 kg CO_2-eq and 9.1 kg

CO_2-eq for integrated and redissolution spinning, respectively, highlighting the importance of alternative sustainable energy sources in decarbonising advanced materials production.

The environmental impact indicates high sensitivity to ionic liquid synthesis (see Fig. S12 in the ESI†). It is crucial to recycle the ionic liquid at least 10 times, as this reduced GWP impact by 72% and 68% for integrated and redissolution spinning in our model, respectively. Increasing the recycling of the ionic liquid during fractionation from 10 to 50 cycles benefitted the environmental profile of the lignin carbon fibres by generating further GWP savings of ~2% and 3%, respectively. This analysis implies that after 50 recycling cycles (equivalent to a 2% IL loss rate per batch), additional recycling of the ionic liquid would not significantly improve the environmental profile of the lignin carbon fibre.

Cost analysis for ionosolv lignin fibre spinning

Unlike environmental analysis, studies focusing on the economic evaluation of lignin carbon fibre production, especially cradle-to-gate, are rare.[55] The economic performance of the lignin carbon fibre production methods evaluated in this study is shown in Fig. 7. Assumptions made in terms of cost and sales prices are shown in Table S9.† Key costs (in US dollars) are biomass at $90 t^{-1}, PVA at $2.68 kg^{-1} and IL at $0.54 kg^{-1}, and key sale prices are unbleached cellulose at $700 t^{-1}, furfural at $1830 t^{-1}, and acetic acid at $604 t^{-1}.

Using the model, the production cost for integrated spun carbon fibres was calculated to be $9.02 kg^{-1}, and slightly higher, $9.69 kg^{-1}, for redissolution spun fibres. The largest contributions to the total production costs, for both spinning approaches, were operating cost such as utilities, reagents, general overheads, and biomass feedstock, accounting for 58%, 29%, 18.4% and 5.9%, respectively. As expected, energy cost (electricity and natural gas to generate steam) were key contributors. Lignin carbon fibre production required a levelised capital cost of $1.5 kg^{-1} *via* integrated spinning and $1.8 kg^{-1} *via* redissolution spinning (Fig. 7a), showing that lignin carbon fibre production cost is dominated by operating cost, as is expected for bulk material production. The higher capital investment for redissolution spinning is due to the additional production stages. Interestingly, the production costs of the two options are not far apart. This parity is due to the total unit of product (1 kg carbon fibre) being dependent on the carbon yield which was lower for integrated spinning (36.6%) compared to redissolution spun carbon fibres (42%). The results indicate that carbon yield strongly affects the economic performance of the production process; hence future developments should target improving carbon yield in addition to mechanical properties, as concluded by others.[1] Revenue from the sale of the co-products of lignin extraction contributes to the lower cost of the lignin carbon fibres, especially cellulose and furfural, as they help offset processing costs associated with feedstock and lignin isolation. However, reliance on revenue from co-products means that fluctuations in these revenues will indirectly affect lignin carbon fibre production cost.

The costs calculated with our model are similar to the ones estimated by the US Department of Energy 2010 production cost
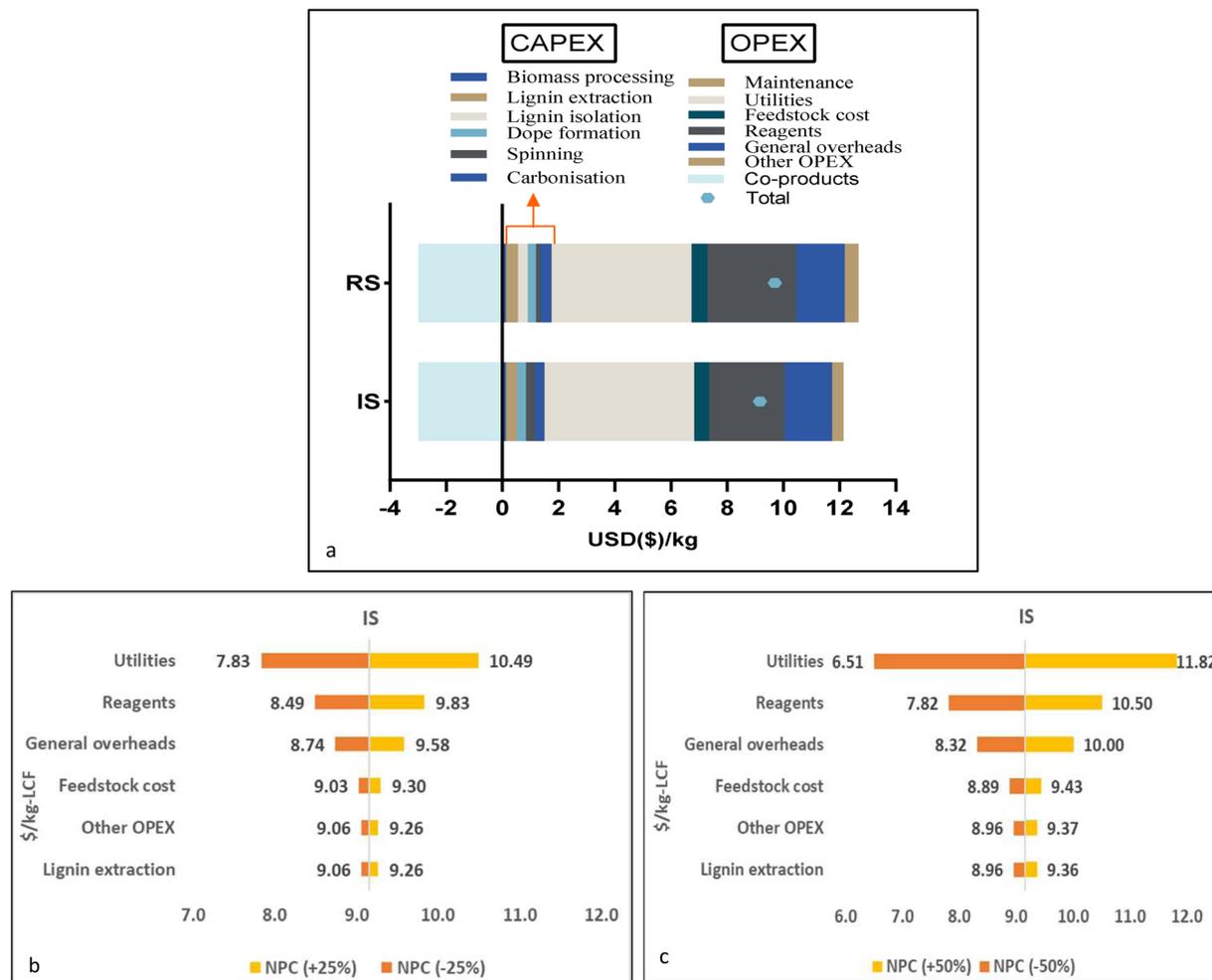
Fig. 7 Cost analysis (base case) for carbon fibre production *via* redissolution (RS) and integrated spinning (IS). (a) Production cost of lignin carbon fibre. (b) and (c) Sensitivity analysis on utility cost (mainly energy), overheads, raw materials, utility cost and feedstock cost for the integrated fibre spinning process.

of $6.27 kg^{-1} ($9.08 kg^{-1} in 2024 accounting for inflation) for lignin carbon fibres at 35% carbon yield.[1] The DoE model indicated that a carbon yield of 55% could reduce the carbon fibre cost further to $4 kg^{-1} ($5.79 kg^{-1} in 2024).[59] The observation that carbon yield has an important influence on carbon fibre price is aligned with this study. Production costs could be reduced further through classical process engineering economies of scale, for example, through capital cost reduction, investment in energy integration, and improved material recovery, especially minimising the amount of water in precursor fibre production.

Literature indicates an average market value of $20 kg^{-1} PAN carbon fibre for a production capacity of 1500 t per year (ref. 60) and $21.5 kg^{-1} (ref. 61) for non-aerospace grade PAN carbon fibres, which is more than double the lignin carbon fibre production modelled here. The DoE predicted $12.25 kg^{-1} for low-grade textile PAN carbon fibres (the lowest performance grade), after cost optimisation in the same model, which is just above the lignin carbon fibre cost found for integrated lignin carbon fibre spinning.[62] The production of the PAN precursor attracts high cost due to the relatively high precursor price (∼$1.4

kg^{-1}), intensive energy use and expensive solvents (∼$3.5 kg^{-1}),[56] while the lignin precursor fibre in this model was produced from low-cost feed biomass ($0.08 kg^{-1}) using a low-cost solvent ($0.53 kg^{-1}), which presents a competitive advantage for lignin carbon fibres against PAN carbon fibres (fossil- and bio-based PAN).

The ionosolv lignin carbon fibres have a similar production cost to proposed fossil-derived low-cost carbon fibres. For low-cost fossil-based sources such as asphaltene, production costs of $10.16 kg^{-1} carbon fibre for a 3000 tonnes per year production capacity[62] and $10.81 kg^{-1} carbon fibre for a 2140 tonnes per year capacity[60] have been reported. The modelled asphaltene carbon fibre cost was ∼10% higher than the lignin carbon fibres cost obtained in this study, which highlights the potential cost benefits associated with lignin-based carbon fibres.

Four sensitivity scenarios were employed to probe the effect of changes in key cost contributors to the overall lignin carbon fibre cost. The greatest cost sensitivity is to utility cost, which are dominated by electricity and fuel. Fig. 7b and c show that a drop in utility cost by 25% reduced total production cost to $7.83 kg^{-1} and a 25% increase in the utility component raised it to $10.49 kg^{-1} for the integrated spinning process. A larger

(50%) price drop in the utility cost further reduced the total production cost to $6.5 kg^{-1}, highlighting the need for cost-effective sustainable energy sources. Sensitivity plots for the redissolution spinning option follow a similar trend and can be found in Fig. S15 in the ESI.†

The comparisons of cost and environmental impact made on a per kg basis need to be considered in light of the specific performance of the fibres and their potential applications. Significant performance improvements are needed for direct substitution in existing PAN fibre applications, even at lower standard modulus grades; however, more modest improvements could be achieved through the adjustments to fibre spinning processes discussed above, which could introduce lignin-derived carbon fibres into sectors where lower cost and improved environmental profile are beneficial and moderate mechanical properties acceptable. Examples include new applications such as reinforcing conductive building materials and existing applications such as ultrahigh temperature thermal insulation, electrostatic dissipation, and ablative composites.[18]

Conclusions

This study demonstrates a unique process concept for generating sustainable low-cost carbon fibres directly from wood *via* "integrated spinning". The approach is enabled by a low-cost IL–water mixture which extracts lignin from wood feedstocks and is compatible with wet-spinning when poly(vinyl alcohol) is added as a spinning aid. The dope composition and coagulation bath consistently provided desirable circular cross-sections and smooth fibre surfaces with good carbon yields (up to 36.6%) upon fibre pyrolysis. Interestingly, the measured tensile strengths of the carbonised fibres were higher than those observed for similar carbonised fibres obtained *via* re-dissolution spinning;[40] however, they were lower than the current state-of-the art. To improve tensile properties, further fibre engineering is required, such as reduction of fibre diameters and fibre drawing to induce polymer alignment.

The study also established the associated environmental impacts and production cost for integrated spinning in comparison to carbon fibre production using isolating ionosolv lignin. Cradle-to-gate LCA showed that the GWP can be reduced by 18% when switching from redissolution spinning to integrated spinning and is associated with a significant reduction in the eutrophication impact; however, the cost was barely reduced, which our model shows is due to the lower carbon yield obtained for the carbon fibres generated *via* integrated spinning. The TEA showed promising cost reductions for both approaches (<$10 kg^{-1}) which could be improved by increasing carbon fibre yield and production scale. A reduction in stabilisation time to 30 min and the use of recycled ionic liquid (at least 10 times) are needed to achieve the modelled costs and environmental performance. The results motivate future optimisation of carbon fibre performance, for example increasing Young's modulus to >90 GPa, as achieved by high performance glass fibres (HM/T2) and improving carbon fibre yield in

subsequent studies, which could then lead to process development.

Data availability

Data supporting this article have been included as part of the ESI file,† which contains details of the methods used for experimental and modelling work, such as compositional analysis, calculations used to generate dope compositions and measuring the coagulated fibre yield. The file also contains NMR spectra of ionosolv black liquors, additional optical micrographs of solutions, scanning electron micrographs of lignin and carbon fibres, and a discussion of shear viscosity measurements, process flow diagrams, life cycle inventories, cost data, and additional sensitivity analyses. The repository "Integrated fibre spinning" (https://doi.org/10.6084/m9.figshare.29505977) contains a spreadsheet for calculating the integrated spinning dope composition and a spreadsheet summarising the data used for the LCA and TEA.

Author contributions

SMY contributed to this study through methodology development, investigation, formal analysis of the experimental lignin carbon fibre work and visualisation and writing of the first draft. RIM was responsible for investigation, formal analysis, visualisation, writing and editing of the LCA and TEA work. ET contributed methodology development, investigation and formal analysis for the coagulated fibre yield. CBT contributed to formal analysis of lignin dope preparation. NS was responsible for reviewing the LCA and TEA methods and the manuscript. MS contributed to conceptualization, funding acquisition, supervision, writing (review and editing). ABT contributed to conceptualization, funding acquisition, methodology development, supervision, project management, project administration, visualisation and writing (review and editing).

Conflicts of interest

The authors have no conflicts to declare.

Acknowledgements

References

1 D. A. Baker and T. G. Rials, *J. Appl. Polym. Sci.*, 2013, **130**, 713–728.

2 E. Frank, L. M. Steudle, D. Ingildeev, J. M. Spörl and M. R. Buchmeiser, *Angew. Chem., Int. Ed.*, 2014, **53**, 5262–5298.

3 E. M. Karp, T. R. Eaton, V. Sànchez i Nogué, V. Vorotnikov, M. J. Biddy, E. C. D. Tan, D. G. Brandner, R. M. Cywar, R. Liu, L. P. Manker, W. E. Michener, M. Gilhespy, Z. Skoufa, M. J. Watson, O. S. Fruchey, D. R. Vardon, R. T. Gill, A. D. Bratis and G. T. Beckham, *Science*, 2017, **358**, 1307–1310.

4 H. Sixta, *Handbook of Pulp*, Wiley-VCH Verlag GmbH & Co. KGaA, 2006.

5 H. Wang, Y. Pu, A. Ragauskas and B. Yang, *Bioresour. Technol.*, 2019, **271**, 449–461.

6 A. J. Ragauskas, G. T. Beckham, M. J. Biddy, R. Chandra, F. Chen, M. F. Davis, B. H. Davison, R. A. Dixon, P. Gilna, M. Keller, P. Langan, A. K. Naskar, J. N. Saddler, T. J. Tschaplinski, G. A. Tuskan and C. E. Wyman, *Science*, 2014, 344.

7 F. Souto and V. Calado, *Green Chem.*, 2022, **24**, 8172–8192.

8 R. Rinaldi, R. Jastrzebski, M. T. Clough, J. Ralph, M. Kennema, P. C. A. Bruijnincx and B. M. Weckhuysen, *Angew. Chem., Int. Ed.*, 2016, **55**, 8164–8215.

9 A. A. Ogale, M. Zhang and J. Jin, *J. Appl. Polym. Sci.*, 2016, **133**, 43974–43807.

10 V. D. Obasa, O. A. Olanrewaju, O. P. Gbenebor, E. F. Ochulor, C. C. Odili, Y. O. Abiodun and S. O. Adeosun, *Atmosphere*, 2022, **13**, 1605.

11 W. Qu, J. Yang, X. Sun, X. Bai, H. Jin and M. Zhang, *Int. J. Biol. Macromol.*, 2021, **189**, 768–784.

12 J. Jin, J. Ding, A. Klett, M. C. Thies and A. A. Ogale, *ACS Sustain. Chem. Eng.*, 2018, **6**, 14135–14142.

13 A. Bengtsson, P. Hecht, J. Sommertune, M. Ek, M. Sedin and E. Sjöholm, *ACS Sustain. Chem. Eng.*, 2020, **8**, 6826–6833.

14 M. Culebras, A. Beaucamp, Y. Wang, M. M. Clauss, E. Frank and M. N. Collins, *ACS Sustain. Chem. Eng.*, 2018, **6**, 8816–8825.

15 M. Vaughan, A. Beaucamp and M. N. Collins, *Composites, Part B*, 2025, **292**, 112024.

16 Y. Luo, M. E. A. Razzaq, W. Qu, A. A. B. A. Mohammed, A. Aui, H. Zobeiri, M. M. Wright, X. Wang and X. Bai, *Green Chem.*, 2024, **26**, 3281–3300.

17 J. F. Kadla and S. Kubo, *Composites, Part A*, 2004, **35**, 395–400.

18 S. V. Kanhere, B. Lynn, M. C. Thies and A. A. Ogale, *RSC Sustain.*, 2024, **2**, 2357–2366.

19 P. Kreis, E. Frank, B. Clauß, V. Bauch, H. Stolpmann, L. Kuske, T. Schneck, S. König and M. R. Buchmeiser, *Macromol. Mater. Eng.*, 2024, **309**, 2300296.

20 D. A. Baker, N. C. Gallego and F. S. Baker, *J. Appl. Polym. Sci.*, 2012, **124**, 227–234.

21 W. Qu, J. Liu, Y. Xue, X. Wang and X. Bai, *J. Appl. Polym. Sci.*, 2018, **135**, 45736.

22 L. M. Steudle, E. Frank, A. Ota, U. Hageroth, S. Henzler, W. Schuler, R. Neupert and M. R. Buchmeiser, *Macromol. Mater. Eng.*, 2017, **302**, 1600441.

23 W. Qin and J. F. Kadla, *J. Appl. Polym. Sci.*, 2012, **126**, E204–E213.

24 K. Sudo and K. Shimizu, *J. Appl. Polym. Sci.*, 1992, **44**, 127–134.

25 O. Hosseinaei, D. P. Harper, J. J. Bozell and T. G. Rials, *Int. J. Mol. Sci.*, 2017, **18**, 1410.

26 M. Föllmer, S. Jestin, W. Neri, V. S. Vo, A. Derré, C. Mercader and P. Poulin, *Adv. Sustainable Syst.*, 2019, **3**, 1900082.

27 J. F. Kadla, S. Kubo, R. A. Venditti, R. D. Gilbert, A. L. Compere and W. Griffith, *Carbon*, 2002, **40**, 2913–2920.

28 X. Jiang, Q. Ouyang, D. Liu, J. Huang, H. Ma, Y. Chen, X. Wang and W. Sun, *Holzforschung*, 2018, **72**, 727–734.

29 A. Brandt, J. Grasvik, J. P. Hallett and T. Welton, *Green Chem.*, 2013, **15**, 550–583.

30 W.-C. Tu, L. Weigand, M. Hummel, H. Sixta, A. Brandt-Talbot and J. P. Hallett, *Cellulose*, 2020, **27**, 4745–4761.

31 A. Brandt, L. Chen, B. E. van Dongen, T. Welton and J. P. Hallett, *Green Chem.*, 2015, **17**, 5019–5034.

32 H. Baaqel, I. Díaz, V. Tulus, B. Chachuat, G. Guillén-Gosálbez and J. P. Hallett, *Green Chem.*, 2020, **22**, 3132–3140.

33 A. Brandt-Talbot, F. J. V. Gschwend, P. S. Fennell, T. M. Lammens, B. Tan, J. Weale and J. P. Hallett, *Green Chem.*, 2017, **19**, 3078–3102.

34 A. R. Abouelela, S.-y. Tan, G. H. Kelsall and J. P. Hallett, *ACS Sustain. Chem. Eng.*, 2020, **8**, 14441–14461.

35 F. J. V. Gschwend, C. L. Chambon, M. Biedka, A. Brandt-Talbot, P. S. Fennell and J. P. Hallett, *Green Chem.*, 2019, **21**, 692–703.

36 F. Malaret, F. J. V. Gschwend, J. M. Lopes, W.-C. Tu and J. P. Hallett, *RSC Adv.*, 2020, **10**, 16050–16060.

37 C. L. Chambon, M. Chen, P. S. Fennell and J. P. Hallett, *Front. Chem.*, 2019, 7.

38 C. Guizani, S. Larkiala, K. Moriam, D. Sawada, S. Elsayed, S. Rantasalo, M. Hummel and H. Sixta, *J. Appl. Polym. Sci.*, 2021, **138**, 49787.

39 M. Morales, PhD thesis, ETH Zürich, 2016.

40 S. M. Yang, M. S. P. Shaffer and A. Brandt-Talbot, *ACS Sustain. Chem. Eng.*, 2023, **11**, 8800–8811.

41 E. Chiellini, A. Corti, S. D'Antone and R. Solaro, *Prog. Polym. Sci.*, 2003, **28**, 963–1014.

42 E. Dickinson, M. Harrison, M. Parker, M. Dickinson, J. Donarski, A. Charlton, R. Nolan, A. Rafat, F. Gschwend, J. Hallett, M. Wakefield and J. Wilson, *PLoS One*, 2019, **14**, e0224771.

43 *Statista, Distribution of demand for chemical pulp worldwide in 2021, by Grade*, https://www.statista.com/statistics/596455/global-demand-distribution-for-chemical-30-pulp-by-grade, accessed 2025, 12 june.

44 J. Sluiter and A. Sluiter, *Summative Mass Closure: Laboratory Analytical Procedure (LAP) Review and Integration: Feedstocks (Revised July 2011)*, NREL, 2011.

45 F. J. V. Gschwend, A. Brandt, C. L. Chambon, W.-C. Tu, L. Weigand and J. P. Hallett, *JoVE*, 2016, e54246, DOI: 10.3791/54246.

46 A. Sluiter, B. Hames, R. Ruiz, C. Scarlata, J. Sluiter, D. Templeton and D. Crocker, *National Renewable Energy Laboratory*, U.S. Department of Energy, 2012.

47 *ISO 14044:2006 Standard: Environmental management - Life cycle assessment - Requirements and guidelines*, **https://www.iso.org/standard/38498.html**.

48 C. L. Chambon, P. Verdía, P. S. Fennell and J. P. Hallett, *Sci. Rep.*, 2021, **11**, 15383.

49 F. J. V. Gschwend, F. Malaret, S. Shinde, A. Brandt-Talbot and J. P. Hallett, *Green Chem.*, 2018, **20**, 3486–3498.

50 A. R. Abouelela, F. V. Gschwend, F. Malaret and J. P. Hallett, in *Commercial Applications of Ionic Liquids*, ed. M. B. Shiflett, Springer International Publishing, Cham, 2020, pp. 87–127, DOI: **10.1007/978-3-030-35245-5_5**.

51 N.-D. Le, M. Trogen, R. J. Varley, M. Hummel and N. Byrne, *Biomacromolecules*, 2022, **23**, 839–846.

52 A. Bengtsson, J. Bengtsson, M. Sedin and E. Sjöholm, *ACS Sustain. Chem. Eng.*, 2019, **7**, 8440–8448.

53 F.-X. Collard and J. Blin, *Renewable Sustainable Energy Rev.*, 2014, **38**, 594–608.

54 S.-C. Shi and T.-H. Chen, *Front. Mater.*, 2023, **10**.

55 D. G. Kulas, M. C. Thies and D. R. Shonnard, *ACS Sustain. Chem. Eng.*, 2021, **9**, 5388–5395.

56 A. Dér, N. Dilger, A. Kaluza, C. Creighton, S. Kara, R. Varley, C. Herrmann and S. Thiede, *J. Cleaner Prod.*, 2021, **303**, 127105.

57 M. Janssen, E Gustafsson, L Echardt, J. Wallinder and J. Wolf, Life cycle assessment of lignin-based carbon fibres, *14th Conference on Sustainable Development of Energy, Water and Environment Systems: (SDEWES), Presented at the 14th Conference on sustainable development of energy, water and environment systems (SDEWES)*, Dubrovnik, 1–6 October, 2019.

58 A. Beaucamp, Y. Wang, M. Culebras and M. N. Collins, *Green Chem.*, 2019, **21**, 5063–5072.

59 T. M. Prenzel, A. Hohmann, T. Prescher, K. Angerer, D. Wehner, R. Ilg, T. von Reden, K. Drechsler and S. Albrecht, *Polymers*, 2024, **16**, 12.

60 S. Nunna, P. Blanchard, D. Buckmaster, S. Davis and M. Naebe, *Heliyon*, 2019, **5**, e02698.

61 N. Shama Rao, T. G. A. Simha, K. P. Rao. and G. V. V. Ravi Kumar, *Carbon Composites Are Becoming Competitive and Cost-Effective*, White Paper, 2018.

62 M. Baritto, A. O. Oni and A. Kumar, *J. Cleaner Prod.*, 2023, **428**, 139489.